
This copy is for your personal, non-commercial use only.

If you wish to distribute this article to others, you can order high-quality copies for your colleagues, clients, or customers by [clicking here](#).

Permission to republish or repurpose articles or portions of articles can be obtained by following the guidelines [here](#).

The following resources related to this article are available online at www.sciencemag.org (this information is current as of August 28, 2011):

Updated information and services, including high-resolution figures, can be found in the online version of this article at:

<http://www.sciencemag.org/content/326/5955/959.full.html>

Supporting Online Material can be found at:

<http://www.sciencemag.org/content/suppl/2009/10/15/1180906.DC1.html>

A list of selected additional articles on the Science Web sites **related to this article** can be found at:

<http://www.sciencemag.org/content/326/5955/959.full.html#related>

This article **cites 28 articles**, 6 of which can be accessed free:

<http://www.sciencemag.org/content/326/5955/959.full.html#ref-list-1>

This article has been **cited by** 11 article(s) on the ISI Web of Science

This article has been **cited by** 4 articles hosted by HighWire Press; see:

<http://www.sciencemag.org/content/326/5955/959.full.html#related-urls>

This article appears in the following **subject collections**:

Planetary Science

http://www.sciencemag.org/cgi/collection/planet_sci

Global Observations of the Interstellar Interaction from the Interstellar Boundary Explorer (IBEX)

D. J. McComas,^{1,2*} F. Allegrini,^{1,2} P. Bochsler,³ M. Bzowski,⁴ E. R. Christian,⁵ G. B. Crew,⁶ R. DeMajistre,⁷ H. Fahr,⁸ H. Fichtner,⁹ P. C. Frisch,¹⁰ H. O. Funsten,¹¹ S. A. Fuselier,¹² G. Gloeckler,¹³ M. Gruntman,¹⁴ J. Heerikhuisen,¹⁵ V. Izmodenov,^{16,17,18} P. Janzen,¹⁹ P. Knappenberger,²⁰ S. Krimigis,^{7,21} H. Kucharek,²² M. Lee,²² G. Livadiotis,¹ S. Livi,^{1,2} R. J. MacDowall,⁵ D. Mitchell,⁷ E. Möbius,²² T. Moore,⁵ N. V. Pogorelov,¹⁵ D. Reisenfeld,¹⁹ E. Roelof,⁷ L. Saul,³ N. A. Schwadron,²³ P. W. Valek,^{1,2} R. Vanderspek,⁶ P. Wurzel,³ G. P. Zank¹⁵

The Sun moves through the local interstellar medium, continuously emitting ionized, supersonic solar wind plasma and carving out a cavity in interstellar space called the heliosphere. The recently launched Interstellar Boundary Explorer (IBEX) spacecraft has completed its first all-sky maps of the interstellar interaction at the edge of the heliosphere by imaging energetic neutral atoms (ENAs) emanating from this region. We found a bright ribbon of ENA emission, unpredicted by prior models or theories, that may be ordered by the local interstellar magnetic field interacting with the heliosphere. This ribbon is superposed on globally distributed flux variations ordered by both the solar wind structure and the direction of motion through the interstellar medium. Our results indicate that the external galactic environment strongly imprints the heliosphere.

The Sun continuously emits ionized solar wind that flows supersonically outward at ~ 300 to 800 km s^{-1} until it reaches the termination shock (TS), where it slows and compresses. This flow inflates a bubble in the local interstellar medium (LISM) called the heliosphere. The heliosphere moves through the LISM at $\sim 26 \text{ km s}^{-1}$, so the LISM plasma dynamic pressure pushes the boundary between the solar wind and the LISM (the heliopause) in at the nose and presumably forms a tail in the opposite direction. The solar wind also contains interstellar pickup ions (PUIs) with energies of a

few keV/amu, produced by ionization of cold interstellar neutrals that drift into the heliosphere. At the TS, hydrogen PUIs, whose number density is 10 to 20% that of the solar wind, are heated, producing a suprathermal population of ions. These ions dominate the pressure in the inner heliosheath, which lies between the TS and heliopause. Energetic neutral atoms (ENAs) are generated in this region when low-energy [few electron volts (eV)] interstellar neutrals undergo charge exchange with either solar wind ions or PUIs (1–4). Once produced, the ENAs move freely across magnetic fields that confine the plasma ions, and some small fraction propagate all the way into Earth orbit where they can be detected.

NASA's Interstellar Boundary Explorer (IBEX) (5) is dedicated to imaging ENAs propagating in from the far reaches of the outer heliosphere. IBEX was launched 19 October 2008 and subsequently maneuvered into a high-altitude, highly elliptical ($\sim 15,000 \times 300,000 \text{ km}$), roughly week-long orbit. IBEX carries two high-sensitivity, single-pixel ENA cameras: IBEX-Lo (6) measures ENAs from $\sim 10 \text{ eV}$ to 2 keV , while IBEX-Hi (7) measures them from $\sim 300 \text{ eV}$ to 6 keV . Over this broad energy range, IBEX measures H ENAs arising from charge exchange with both the slower solar wind ions ($< \sim 1 \text{ keV}$) and PUIs (~ 1 to a few keV).

Over the first half of 2009, IBEX built up its first global, energy-resolved maps of ENAs coming in from the outer heliosphere (5); these maps generally reflect the solar minimum conditions that have persisted for the past several years. In addition to the all-sky maps and energy spectra, IBEX also made direct observations of interstellar H and O from the LISM (8). These

observations allow us to differentiate various particle populations, providing information about the interaction of the heliosphere with the LISM and about the interstellar environment itself.

Voyager 1 (9) and later Voyager 2 (10) crossed the TS and are making in situ measurements along two paths in the inner heliosheath. In contrast, IBEX's energy-resolved maps reveal the global interstellar interaction in all directions. The most striking feature in the IBEX sky maps is an unexpected, bright, narrow ribbon of ENA emissions that snakes between the directions of the Voyagers. This feature was not predicted by any model or theory, so interpreting the IBEX observations will require the development of a new understanding of the heliospheric interaction with the LISM.

The IBEX all-sky maps (Fig. 1) show that ENA fluxes vary over the ribbon, with maxima 2 to 3 times brighter than the surrounding regions. The ribbon is variable in width from $< 15^\circ$ to $> 25^\circ$ full width at half maximum (11), contains fine structure (Fig. 1B), and passes $\sim 25^\circ$ away from the heliospheric nose. The ribbon has brighter emissions from somewhat broader regions at higher latitudes in both hemispheres ($\sim 60^\circ\text{N}$ and $\sim 40^\circ\text{S}$), with the former having a different spectral shape than the rest of the ribbon (12). Although not optimally shown in these projections, the ribbon weakens but also extends back behind the northern pole, nearly closing a loop on the sky (12).

IBEX-Lo observations independently confirm the ribbon in the overlapping energy range (Fig. 1H) and extend down to $\sim 200 \text{ eV}$ (Fig. 1G). The ribbon is observed from there up to $> 6 \text{ keV}$, the top of the IBEX-Hi energy range (Fig. 1F), with the highest relative intensity at $\sim 1 \text{ keV}$ (11). Additional observations from Cassini/INCA (13) indicate that some portions of the ribbon may extend to even higher energies. Finally, although observations of the ribbon collected 6 months apart ($\sim 0^\circ$, $\sim 180^\circ$ ecliptic longitudes) indicate that it remained a largely stable structure during this period, these observations also suggest the possibility of some temporal evolution.

The power-law spectral slopes of the ENA flux (κ) display broad variations across the sky (Fig. 2) that are ordered by ecliptic latitude and longitude (i.e., the interstellar flow direction). These observations are generally consistent with the concept that ENAs are produced from TS-heated, nonthermal plasma throughout the inner heliosheath. The spectrum is flatter (lower κ) near the poles relative to the equator; this might be caused by the faster solar wind at higher latitudes, which generates and entrains substantially higher-energy PUIs than near the ecliptic. The spectra toward the tail are steeper ($\kappa > 2$) than near the nose ($\kappa \approx 1.5$), possibly owing to longer line-of-sight (LOS) integrations of low-energy ions toward the tail. Remarkably, the ribbon is barely visible in this spectral slope map, even though the fluxes are several times higher.

¹Southwest Research Institute, San Antonio, TX 78228, USA.

²University of Texas, San Antonio, TX 78249, USA. ³Physikalisches Institut, University of Bern, CH-3012 Bern, Switzerland.

⁴Space Research Centre of the Polish Academy of Sciences, 00-716 Warsaw, Poland. ⁵NASA Goddard Space Flight Center, Greenbelt, MD 20771, USA. ⁶Massachusetts Institute of Technology, Cambridge, MA 02139, USA. ⁷Applied Physics Laboratory, Johns Hopkins University, Laurel, MD 20723, USA.

⁸University of Bonn, 53115 Bonn, Germany. ⁹Ruhr-Universität Bochum, 44780 Bochum, Germany. ¹⁰University of Chicago, Chicago, IL 60637, USA. ¹¹Los Alamos National Laboratory, Los Alamos, NM 87545, USA. ¹²Lockheed Martin Advanced Technology Center, Palo Alto, CA 94304, USA. ¹³University of Michigan, Ann Arbor, MI 48109, USA. ¹⁴University of Southern California, Los Angeles, CA 90089, USA. ¹⁵University of Alabama, Huntsville, AL 35805, USA. ¹⁶Moscow State University, 119899 Moscow, Russia. ¹⁷Space Research Institute (IKI), Russian Academy of Sciences, 117997 Moscow, Russia. ¹⁸Institute for Problems in Mechanics, Russian Academy of Sciences, 117526 Moscow, Russia. ¹⁹University of Montana, Missoula, MT 59812, USA. ²⁰Adler Planetarium, Chicago, IL 60605, USA. ²¹Office for Space Research and Technology, Academy of Athens, 106 79 Athens, Greece. ²²Space Science Center, University of New Hampshire, Durham, NH 03824, USA. ²³Boston University, Boston, MA 02215, USA.

*To whom correspondence should be addressed. E-mail: dmcomas@swri.org

As an example of the detailed spectral information provided by IBEX, Fig. 3 shows the ENA energy spectra along LOSs toward the two Voyager spacecraft. These spectra are nearly straight power laws with slopes of ~ 1.5 (Voyager 1) and ~ 1.6 (Voyager 2). Globally, the spectra generally show simple power laws near the equator with distinct enhancements at several keV at higher latitudes (12), again consistent with higher-energy PUIs in the high-latitude, fast solar wind. IBEX observations are consistent with upper bounds on ENA flux based on Ly- α absorption (14). Claims of heliospheric ENA measurements from ASPERA-3 (15) are inconsistent with IBEX observations.

The discovery of the ribbon, not ordered by ecliptic coordinates or the interstellar flow, requires reconsideration of our fundamental concepts of the heliosphere-LISM interaction. A possible explanation could be based on the idea that the local interstellar magnetic field plays a central role in shaping the outer heliosphere. Figure 4 shows a concept for the interaction where the external dynamic and magnetic forces are comparable. Here we depict the external field (16) wrapping around and compressing the heliopause in a way that pushes in the southern hemisphere (17) enough to explain why Voyager 2 crossed the TS ~ 10 AU closer to the Sun (10) than did Voyager 1 (9), once the effects of the decreasing solar wind dynamic pressure inside the TS (18) are included (19). The ribbon closely matches locations where a model (20) using this external field orientation indicates that just outside the heliopause, the field is transverse to IBEX's radial-viewing LOSs (21).

Several factors could contribute to the substantially enhanced emission in the ribbon, including higher energetic ion intensities along the LOS and pitch-angle distributions of ions that preferentially emit radially inward. The combination of the external plasma dynamic (i.e., ram) and magnetic ($\mathbf{J} \times \mathbf{B}$) forces produces a localized band of maximum total pressure around the heliopause, which is substantially offset from the nose for a strong external field (21). Because the suprathermal plasma observed in the inner heliosheath is subsonic, information about the enhanced pressure at the heliopause propagates throughout the inner heliosheath, adjusting the plasma properties and bulk flow and potentially affecting the TS. Flows at the Voyager locations appear to be more directed away from the ribbon than away from the nose. At Voyager 2 (22), south and offset from the nose meridian (Fig. 1), in radial-tangential-normal (RTN) coordinates, $\langle V_T \rangle \sim +48 \text{ km s}^{-1}$, whereas $\langle V_N \rangle$ is only $\sim -14 \text{ km s}^{-1}$. At Voyager 1, northward of the nose, only V_R and V_T were measured (23), but $\langle V_T \rangle \sim -40 \text{ km s}^{-1}$. Thus, the ribbon might indicate the true region of highest pressure in the inner heliosheath. If so, the location of the ribbon divides inner heliosheath flows down the two sides of the heliotail, analogous to a continental divide; this may explain why V_T is

several times V_N at Voyager 2, as well as the large transverse flow at Voyager 1.

If the pressure maximum is aligned with the ribbon and the heliosheath flows are away from it, then this represents the stagnation flow region, where inside the heliopause the radial outflow must go to zero. In this region, the plasma density should maximize, producing copious ENAs that would naturally map the region of maximum pressure. This additional pressure might also ex-

trude a region of the heliopause, forming a spatially limited outward bulge with high density and little bulk flow. Because of the narrow angular extent of the ribbon, it might be expected that the emission region could be radially narrow also, which would require magnetic or some other sort of plasma confinement. Furthermore, the spectral slope of the ribbon is similar to that of the surrounding regions, which suggests that this feature is not dominated by dynamical effects

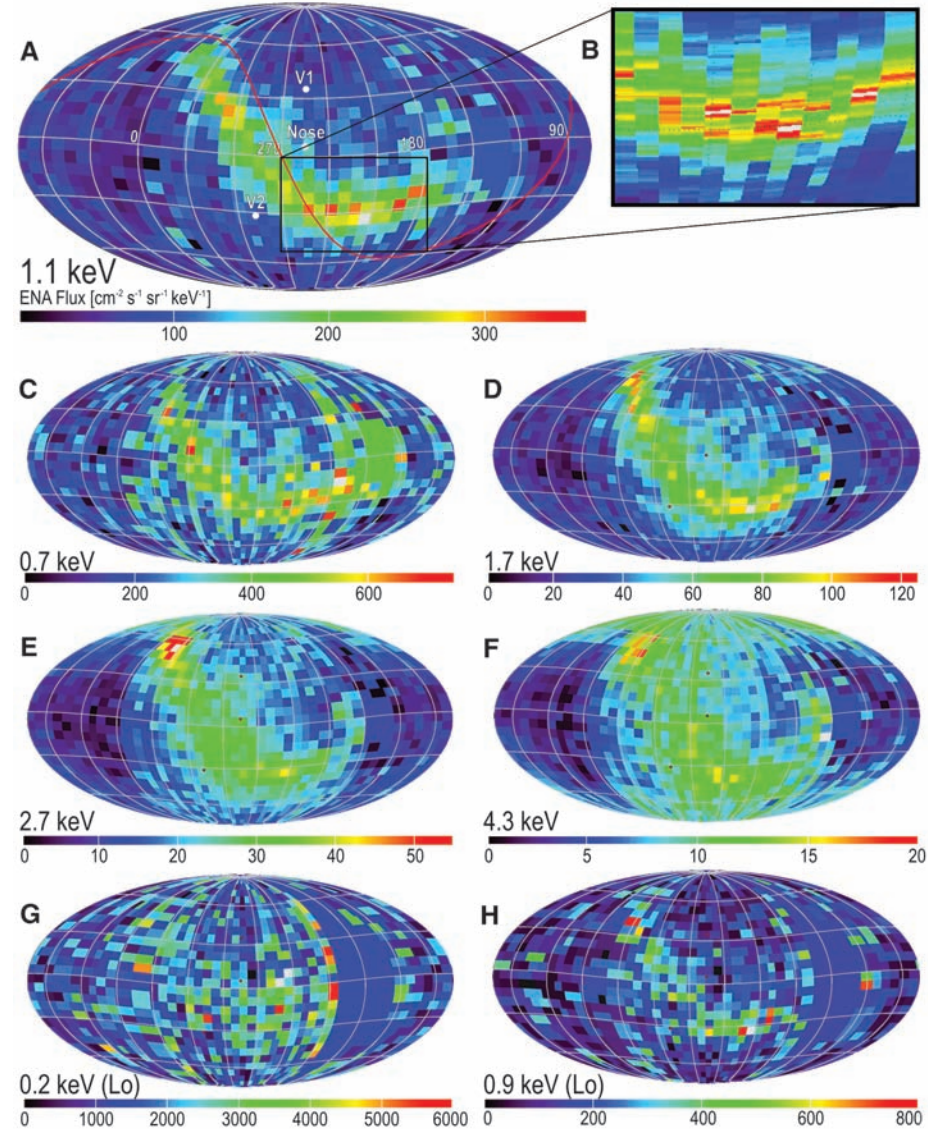


Fig. 1. IBEX all-sky maps of measured ENA fluxes in Mollweide projections in ecliptic coordinates (J2000), where the heliospheric nose is near the middle and the tail extends along both sides. The pixels are 6° in spin phase (latitude), with widths (longitude) determined by the spacecraft pointing for different orbits. Maps are shown in the spacecraft frame for passband central energies from IBEX-Hi of (A) 1.1 keV, (C) 0.7 keV, (D) 1.7 keV, (E) 2.7 keV, and (F) 4.3 keV, and from IBEX-Lo of (G) 0.2 keV and (H) 0.9 keV. Also shown in (A) is the galactic plane (red curve), which clearly does not coincide with the ribbon, as well as directions toward Voyager 1 (V1) ($35^\circ, 255^\circ$), Voyager 2 (V2) ($-32^\circ, 289^\circ$), and the nose ($5^\circ, 255^\circ$). (B) Magnified section of the ribbon where each 0.5° in spin phase is averaged with nearest neighbors to reach 100 counts (10 counts standard deviation). Because of contamination of ENAs from Earth's magnetosphere, a small region on the right side of each map was not sampled in the first 6 months of data; these regions have been filled in with average values from the adjacent areas and appear unpixelated.

Downloaded from www.sciencemag.org on August 28, 2011

(e.g., different energization processes at the TS or elsewhere) but simply reflects the accumulation of particles. Integration of our measured distri-

butions of ENAs over energy suggests that the pressure in the ribbon is considerably higher than in the rest of the sky (12); nonetheless, a region

only ~30 to 60 AU thick could still be in rough pressure balance with the combined external dynamic and magnetic forces (21).

Fig. 2. Sky map, in ecliptic coordinates, of the average power-law spectral slope (κ) from ~0.5 to 6 keV using IBEX-Hi channels 2 to 6. The measurements were transformed into the rest frame of the Sun; unlike Fig. 1, the unsampled region is left black in this image. Although statistical uncertainty remains in individual 6° pixels, global variations are clearly evident.

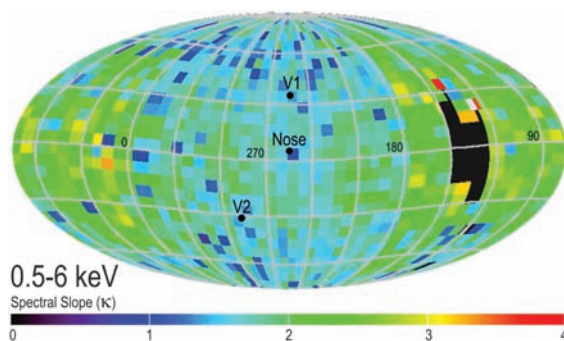


Fig. 3. Energy spectra for 20° × 20° regions centered on the Voyager 1 (thick lines) and Voyager 2 (thin lines) directions. Pre-launch cross-calibration of the IBEX-Lo (red) and -Hi (blue) sensors simultaneously in a single chamber produces quantitative matching between the spectra. Error bars show counting statistics plus likely systematic errors of ±20% for IBEX-Hi and ±30% for IBEX-Lo.

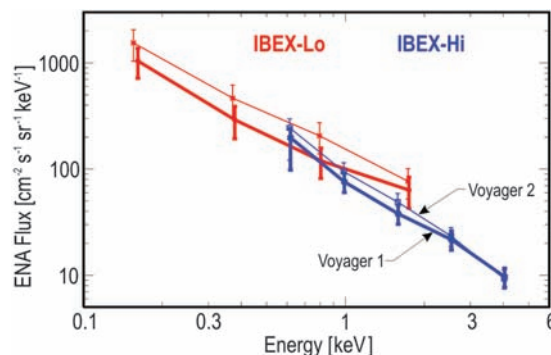
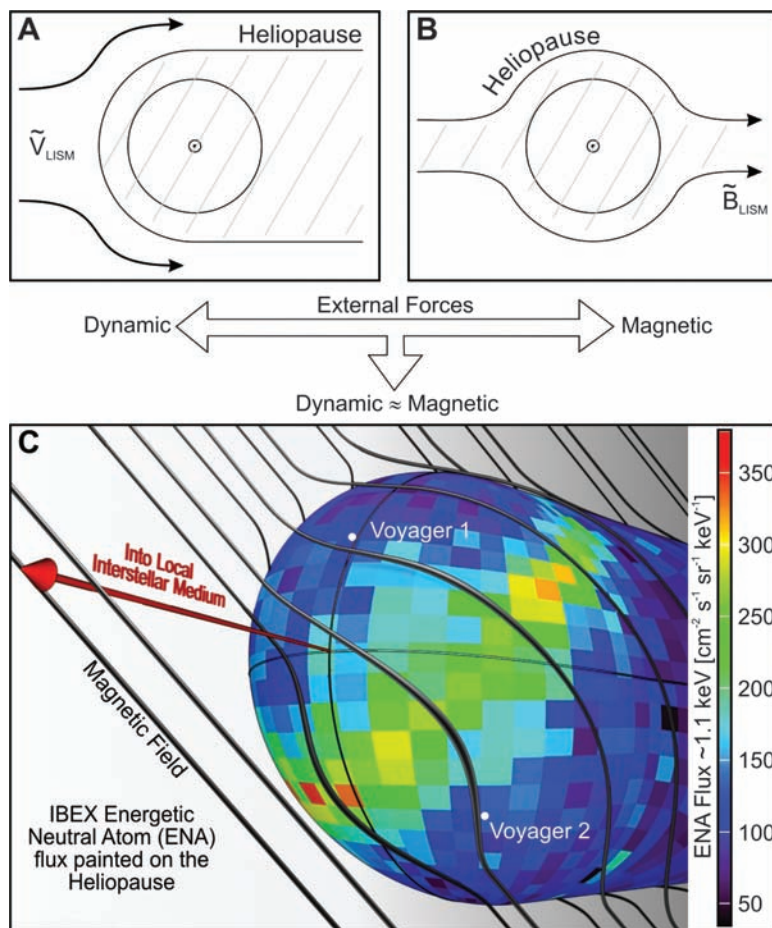


Fig. 4. Schematic diagrams of Parker’s limiting cases for the heliospheric interaction (28). (A) “Hydrodynamic” interaction, where the external dynamic forces \gg magnetic forces. (B) “Diamagnetic cavity” interaction, where the external magnetic forces \gg dynamic forces. (C) Schematic showing an intermediate case, where the external magnetic and dynamic forces are comparable. The measured flux at ~1.1 keV is superposed on the heliopause; the ribbon appears to correlate with where the field is most strongly curved around it.



Another way to trap hot, inner-heliosheath plasma in a relatively narrow structure might be via large-scale, Rayleigh-Taylor-like instabilities (24), which can be driven by neutrals and destabilize the heliopause. Some models show large, semicoherent structures with higher ion densities and sizes greater than tens of AU, moving tailward at <60 km/s along the heliopause (25). Magnetic reconnection across the heliopause would also allow suprathermal heliosheath ions out into the cooler, denser outer heliosheath, potentially confining them in narrow structures. For any method that traps hot plasma farther out beyond the heliopause, expected higher densities of interstellar neutrals there would also enhance ENA production.

Another possible ENA source is from outside the heliopause, where compression of the external field would both enhance densities and provide perpendicular heating to produce more perpendicular ion pitch-angle distributions (21). Such ions preferentially emit ENAs where the LOS is transverse to the interstellar magnetic field. A possible source of ENAs could be fast neutrals emitted from the inner heliosheath, which become ionized just outside the heliopause and then reneutralize, emitting back inward pref-

erentially where the field is perpendicular to IBEX's radial LOS. A simulation including this effect but using only isotropic distributions showed a weak ENA signal (2). Producing a strong, narrow feature would require the PUIs to remain a ring distribution, in the face of instabilities, long enough for many to neutralize. It is also possible that the ribbon ENAs come from inside the TS, perhaps from shock-accelerated PUIs (26) propagating inward through the region where the solar wind decelerates by $\sim 20\%$ over ~ 10 AU, just inside the shock (27).

The brightest regions of the ribbon occur well away from the nose and at latitudes where the slow and fast solar winds interact, forming corotating interaction regions. This suggests that the emissions in the ribbon are at least partially related to the solar wind properties as well as to the external environment. Additionally, although the ribbon appears as a continuous feature, it could be a string of more localized, overlapping "knots" of emission. Certainly other ideas need to be examined, and while our data support some earlier

ideas, in other areas a completely new paradigm is needed for understanding the interaction between our heliosphere and the galactic environment.

References and Notes

- H. Fahr *et al.*, *Rev. Geophys.* **45**, RG4003 (2007).
- V. V. Izmodenov *et al.*, *Space Sci. Rev.* **146**, 329 (2009).
- M. A. Lee *et al.*, *Space Sci. Rev.* **146**, 275 (2009).
- G. P. Zank *et al.*, *Space Sci. Rev.* **146**, 295 (2009).
- D. J. McComas *et al.*, *Space Sci. Rev.* **146**, 11 (2009).
- S. A. Fuselier *et al.*, *Space Sci. Rev.* **146**, 117 (2009).
- H. O. Funsten *et al.*, *Space Sci. Rev.* **146**, 75 (2009).
- E. Möbius *et al.*, *Science* **326**, 969 (2009); published online 15 October 2009 (10.1126/science.1180971).
- E. C. Stone *et al.*, *Science* **309**, 2017 (2005).
- E. C. Stone *et al.*, *Nature* **454**, 71 (2008).
- S. A. Fuselier *et al.*, *Science* **326**, 962 (2009); published online 15 October 2009 (10.1126/science.1180981).
- H. O. Funsten *et al.*, *Science* **326**, 964 (2009); published online 15 October 2009 (10.1126/science.1180927).
- S. M. Krimigis, D. G. Mitchell, E. C. Roelof, K. C. Hsieh, D. J. McComas, *Science* **326**, 972 (2009); published online 15 October 2009 (10.1126/science.1181079).
- B. E. Wood *et al.*, *Astrophys. J.* **657**, 609 (2007).
- P. Wurz *et al.*, *Astrophys. J.* **683**, 248 (2008).
- R. Lallement *et al.*, *Science* **307**, 1447 (2005).
- M. Opher *et al.*, *Astrophys. J.* **640**, L71 (2006).
- D. J. McComas *et al.*, *Geophys. Res. Lett.* **35**, L18103 (2008).
- H. Washimi *et al.*, *Astrophys. J.* **670**, L139 (2007).
- N. V. Pogorelov *et al.*, *Astrophys. J.* **695**, L31 (2009).
- N. A. Schwadron *et al.*, *Science* **326**, 966 (2009); published online 15 October 2009 (10.1126/science.1180986).
- J. D. Richardson *et al.*, *Geophys. Res. Lett.* **36**, L10102 (2009).
- R. B. Decker *et al.*, *AIP Conf. Proc.* **932**, 197 (2007).
- V. B. Baranov *et al.*, *Astron. Astrophys.* **261**, 341 (1992).
- S. N. Borovikov *et al.*, *Astrophys. J.* **682**, 1404 (2008).
- S. V. Chalov, H. J. Fahr, *Astron. Astrophys.* **311**, 317 (1996).
- J. D. Richardson *et al.*, *Nature* **454**, 63 (2008).
- E. N. Parker, *Astrophys. J.* **134**, 20 (1961).
- We thank all the men and women who made the IBEX mission possible. IBEX was primarily funded by NASA as a part of the Explorers Program (contract NNG05EC85C); foreign investigators were supported by their respective national agencies and institutions.

21 August 2009; accepted 2 October 2009

Published online 15 October 2009;

10.1126/science.1180906

Include this information when citing this paper.

Width and Variation of the ENA Flux Ribbon Observed by the Interstellar Boundary Explorer

S. A. Fuselier,^{1*} F. Allegrini,^{2,3} H. O. Funsten,⁴ A. G. Ghielmetti,¹ D. Heitzler,⁵ H. Kucharek,⁵ O. W. Lennartsson,¹ D. J. McComas,^{2,3} E. Möbius,⁵ T. E. Moore,⁶ S. M. Petrinec,¹ L. A. Saul,⁷ J. A. Scheer,⁷ N. Schwadron,⁸ P. Wurz⁷

The dominant feature in Interstellar Boundary Explorer (IBEX) sky maps of heliospheric energetic neutral atom (ENA) flux is a ribbon of enhanced flux that extends over a broad range of ecliptic latitudes and longitudes. It is narrow ($\sim 20^\circ$ average width) but long (extending over 300° in the sky) and is observed at energies from 0.2 to 6 kilo-electron volts. We demonstrate that the flux in the ribbon is a factor of 2 to 3 times higher than that of the more diffuse, globally distributed heliospheric ENA flux. The ribbon is most pronounced at ~ 1 kilo-electron volt. The average width of the ribbon is nearly constant, independent of energy. The ribbon is likely the result of an enhancement in the combined solar wind and pickup ion populations in the heliosheath.

The scientific objective of the Interstellar Boundary Explorer (IBEX) is to discover the global interaction between the Sun's solar wind and the interstellar medium (1). This objective is accomplished through the use of two high-sensitivity neutral atom cameras that detect ENAs from 0.01 to 6 keV. Here, the full energy range of the IBEX payload is used to investigate

average characteristics of the ribbon of enhanced hydrogen flux (Fig. 1) detected by IBEX across a large fraction of the sky (2).

The sky map for 0.2-keV hydrogen [see Fig. 1G in (2)] shows evidence of enhanced 0.2-keV hydrogen flux that generally follows the ribbon seen in Fig. 1. In the 0.2-keV sky map, there is also a high-flux region centered approximately on the ecliptic from roughly the nose direction to -150° longitude. A similar region is evident in a sky map of oxygen (3). These are interstellar oxygen neutrals originating from the nose. The interstellar oxygen is not observed exactly in the nose direction because neutrals are deflected by the Sun's gravity and IBEX measures them in the Earth's reference frame (3). Energetic oxygen neutrals create a hydrogen signature in the IBEX-Lo sensor by knock-off of

negative hydrogen ions from the sensor's neutral-to-negative ion conversion surface (4). Thus, the high-flux region in the 0.2-keV sky map near the nose is not associated with heliospheric hydrogen. Rather, it is a secondary product in the IBEX-Lo sensor from interstellar oxygen. Indeed, sky maps at $E < 0.2$ keV (3) are dominated by the secondary hydrogen flux produced by both interstellar oxygen and helium in the sensor, and it is difficult to identify a ribbon at energies below 0.2 keV. Thus, the ribbon extends from 0.2 to 6 keV [the upper energy of the 4.3-keV sky map in (2)].

To investigate average properties of the ribbon, we integrated the maps at each energy parallel to the thick black curve in Fig. 1 in 6° -wide bins. These integrals define the average cross section profile of the ribbon (Fig. 2A). The ribbon is centered near -3° for all energies, except at 0.2 keV. It is not symmetric about 0° because there is structure in the ribbon at higher angular resolution than shown here (2). The ribbon is a flux enhancement above a more diffuse, globally distributed heliospheric ENA flux (2, 5) (the fluxes at $[-30, -24^\circ]$ and $[24, 30^\circ]$ define the distributed flux). It is most pronounced at 0.9 keV, where it is a factor of 2.3 times more intense than the distributed flux. At both higher and lower energies, the average intensity of the ribbon decreases so that at 0.2 and 2.7 keV, the ribbon flux is only $\sim 25\%$ more intense than the distributed flux. The ribbon is centered in the same location up to 6 keV [the highest IBEX energy; see Fig. 1F in (2)].

At 0.2 keV, the influence of the interstellar neutrals is seen from 12° to 30° . In addition, the ribbon appears to be wider and somewhat displaced from the location at all other energies. Below 0.2 keV, it is difficult to identify a ribbon because hydrogen created in the sensor from

¹Lockheed Martin Advanced Technology Center, Palo Alto, CA 94304, USA. ²University of Texas at San Antonio, San Antonio, TX 78249, USA. ³Southwest Research Institute, San Antonio, TX 78228, USA. ⁴Los Alamos National Laboratory, Los Alamos, NM 87545, USA. ⁵University of New Hampshire, Durham, NH 03824, USA. ⁶Goddard Space Flight Center, Greenbelt, MD 20771, USA. ⁷University of Bern, Physikalisches Institut, 3012 Bern, Switzerland. ⁸Boston University, Boston, MA 02215, USA.

*To whom correspondence should be addressed. E-mail: stephen.a.fuselier@lmco.com